Resistance to Taxol in lung cancer cells associated with increased microtubule dynamics

A. Gonçalves*, D. Braguer*, K. Kamath[†], L. Martello[‡], C. Briand*, S. Horwitz[‡], L. Wilson[†], and M. A. Jordan[†¶]

*Unité Propre de Recherche de l'Enseignement Supérieur-A Centre National de la Recherche Scientifique 6032, Université de la Mediterranée, Marseille, France; [‡]Department of Molecular Pharmacology, Albert Einstein College of Medicine, Bronx, NY 10461; and [†]Department of Molecular, Cellular, and Developmental Biology and Neuroscience Research Institute, University of California, Santa Barbara, CA 93106

Microtubule dynamics are crucial for mitotic spindle assembly and chromosome movement. Suppression of dynamics by Taxol appears responsible for the drug's potent ability to inhibit mitosis and cell proliferation. Although Taxol is an important chemotherapeutic agent, development of resistance limits its efficacy. To examine the role of microtubule dynamics in Taxol resistance, we measured the dynamic instability of individual rhodamine-labeled microtubules in Taxol-sensitive and -resistant living human cancer cells. Taxol-resistant A549-T12 and -T24 cell lines were selected from a human lung carcinoma cell line, A549. They are, respectively, 9- and 17-fold resistant to Taxol and require low concentrations of Taxol for proliferation. We found that microtubule dynamic instability was significantly increased in the Taxol-resistant cells. For example, with A549-T12 cells in the absence of added Taxol, microtubule dynamicity increased 57% as compared with A549 cells. The length and rate of shortening excursions increased 75 and 59%, respectively. These parameters were further increased in A549-T24 cells, with overall dynamicity increasing by 167% compared with parental cells. Thus, the decreased Taxol-sensitivity of these cells can be explained by their increased microtubule dynamics. When grown without Taxol, A549-T12 cells were blocked at the metaphase/anaphase transition and displayed abnormal mitotic spindles with uncongressed chromosomes. In the presence of 2–12 nM Taxol, the cells grew normally, suggesting that mitotic block resulted from excessive microtubule dynamics. These results indicate that microtubule dynamics play an important role in Taxol resistance, and that both excessively rapid dynamics and suppressed dynamics impair mitotic spindle function and inhibit proliferation.

Taxol is a valuable cancer chemotherapeutic agent used for treatment of many types of cancer, including ovary, breast, and lung carcinomas (1). Taxol's principal targets in cells are the spindle microtubules responsible for segregation of duplicated chromosomes to daughter cells at mitosis (2, 3). The drug binds reversibly to tubulin along the surface of microtubules and, at relatively high concentrations in cells, it increases microtubule polymer mass and induces microtubule bundle formation (4). At relatively low concentrations, it strongly suppresses microtubule dynamics, both in cells and in purified microtubule systems, without significantly altering the polymer mass (5, 6). One form of microtubule dynamics that is highly sensitive to Taxol is called dynamic instability, a behavior in which the ends of microtubules undergo frequent stochastic transitions between episodes of growing and shortening. Dynamic instability appears to be essential for progression through mitosis into anaphase. When cells enter mitosis, the interphase array of microtubules is dismantled and a bipolar spindle-shaped array of microtubules displaying rapid dynamic instability is assembled (7, 8). Microtubules emanating from the spindle poles grow and shorten randomly, probing the cytoplasm until they contact and attach to the condensed chromosomes. Attached chromosomes then oscillate under tension toward and away from each spindle pole until all remaining chromosomes attach and congress to the metaphase plate, the metaphase/anaphase checkpoint is satisfied, and anaphase proceeds.

The effects of Taxol on microtubule dynamics have been well studied, both in living cells and with isolated microtubule systems. Its major effects on microtubule dynamic instability are to reduce the rate and extent of microtubule shortening (5, 6). Subtle suppression of microtubule dynamics by Taxol strongly inhibits the assembly and functioning of the mitotic spindle, thereby preventing or slowing cell cycle progression at the metaphase/anaphase checkpoint and eventually inducing cell death (6, 9, 10).

Despite Taxol's success as an antitumor agent, cells usually become resistant to the drug over time, thus severely limiting its long-term effectiveness. Resistance to chemotherapeutic drugs generally, and to Taxol in particular, takes many forms. The best understood mechanism of resistance to Taxol involves the multidrug-resistance phenotype, mediated by the P-glycoprotein efflux pump (11). However, less is known about other resistance mechanisms to Taxol. One mechanism that is likely to cause Taxol resistance is thought to involve alterations in microtubule structure and/or function (12). For example, drug-resistant cancer cell lines and human tumor tissues have been shown to harbor tubulin gene mutations, alterations in total tubulin content, altered microtubule polymer levels, altered expression of tubulin isotypes, and altered microtubule-associated protein expression (13–20). All of these modifications in tubulin could, directly or indirectly, influence microtubule dynamics. Because suppression of microtubule dynamic instability is the event most sensitive to the lowest concentrations of Taxol, we have hypothesized that drug-sensitive and -resistant cells might display altered dynamic instability profiles that could ultimately be responsible for the resistance.

To test this hypothesis, we examined the dynamic instability behavior of individual microtubules in living Taxol-sensitive human lung cancer cells, A549, and their Taxol-resistant subclones, A549-T12 and -T24. These subclones were selected for resistance by continual exposure of the parental cell line to increasing concentrations of Taxol (16). A549-T12 cells are not only 9-fold resistant to Taxol but are also dependent on the presence of low concentrations of the drug (2 nM) for normal growth (16, 21). When grown in Taxol-free medium, these cells are blocked in G_2/M phase, suggesting that Taxol may be required for mitotic spindle function. A549-T24 cells, which are 17-fold resistant to Taxol, also require the presence of low concentrations of Taxol. There are no differences in Taxol accumulation between the parental and the A549-T12 cells (16), suggesting that Taxol-resistance in these cells is P-glycoprotein-independent, and no P-glycoprotein was detected on SDS gels by Western blot.
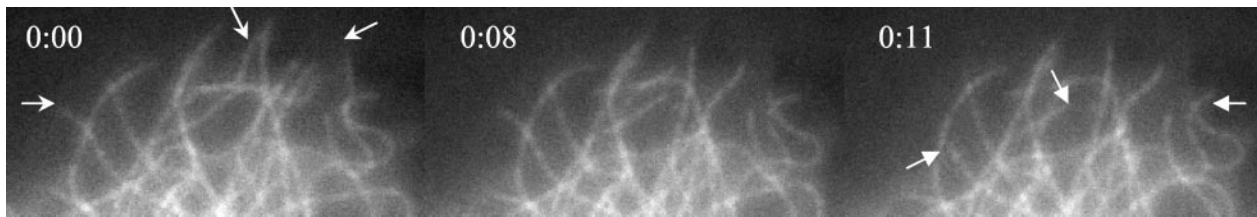
PHARMACOLOGY

Fig. 1. Dynamic behavior of microtubules in living A549 cells. Arrows indicate three microtubules that undergo shortening events. Time is indicated as min:s.

We examined dynamic instability parameters in the parental Taxol-sensitive and the Taxol-resistant cells by digital fluorescence time-lapse microscopy after microinjecting rhodamine-labeled tubulin. We find that the Taxol-resistant cells display significantly enhanced dynamic instability behavior compared with their Taxol-sensitive counterparts, consistent with the decreased Taxol sensitivity of the resistant cells. The Taxol dependence of the resistant cell lines is especially interesting. The data suggest that enhancement of microtubule dynamics is not compatible with normal function. Thus it appears that microtubule dynamics in cells must be maintained in a narrow range for viability.

Materials and Methods

Cell Culture. The human non-small cell lung carcinoma cell line A549, together with its Taxol-resistant derivatives, A549-T12 and A549-T24, were maintained in the absence or presence of Taxol (12 and 24 nM, respectively) (16).

Preparation and Microinjection of Rhodamine Tubulin. Rhodamine tubulin was prepared by carboxymethylrhodamine labeling (Molecular Probes) of microtubules assembled from phosphocellulose-purified bovine brain tubulin (22). The final microtubule pellet was resuspended in cold injection buffer (50 mM potassium glutamate/0.5 mM $MgCl_2$, pH 7.0), centrifuged (35,000 rpm, 15 min, 4°C), and the supernatant was stored at −70°C until use. Cells were seeded in Taxol-free medium 48 h before use at $0.5–1 \times 10^5$ cells/ml on glass coverslips coated with L-polylysine (50 μg/ml), laminin (10 μg/ml), and fibronectin (20 μg/ml). Rhodamine–tubulin (6 mg/ml) was centrifuged to remove aggregates and microinjected by using an Eppendorf Transjector 5246 and Injectman. Injected cells were incubated for 4–6 h (37°C) to allow incorporation of rhodamine–tubulin into microtubules.

Time-Lapse Microscopy and Image Acquisition. Microinjected cells were placed in culture medium lacking sodium bicarbonate and supplemented with 25 mM Hepes/4.5 g/liter glucose/30 μl oxyrase/ml medium Oxyrase (Oxyrase, Mansfield, OH) to reduce photodamage, in a double coverslip chamber, and observed by using a fluorescence inverted microscope (Nikon Eclipse E800) maintained at 37 ± 1°C, with a Nikon plan apochromat 1.4 N.A., ×100 objective lens. Thirty-eight to forty-two images per cell were acquired at 3-s intervals by using a Hamamatsu Orca II (Middlesex, NJ) digital camera driven by METAMORPH software (Universal Imaging, Media, PA).

Analysis of Microtubule Dynamics. The positions of the plus-ends of individual microtubules over time were recorded by using META-MORPH software, exported to Microsoft Excel, and analyzed by using RTM software (23). The lengths of individual microtubules were graphed as a function of time (life histories). Changes in length >0.5 μm were called growth or shortening events. Phases of undetectable changes in length (≦0.5 μm) were called phases of attenuated dynamics or pause. The catastrophe frequency based on time was calculated by dividing the number of transi-

tions from growth or pause to shortening by total time growing and paused. The catastrophe frequency based on length grown was calculated by dividing the number of transitions from growth or pause to shortening by the total distance grown. The rescue frequencies based on distance or time were calculated similarly, dividing the total number of transitions from shortening to growth or pause by the length shortened or the time spent shortening, respectively. Dynamicity is the total length grown and shortened divided by the life span of the microtubule.

Immunofluorescence Microscopy. A549 and A549-T12 cells were plated (5×10^4 cells/ml) on Lab-Tek chamber slides (Nalge Nunc) and incubated for 48 h in the presence or absence of 12 nM Taxol (Calbiochem). Cells were extracted with 0.5% Triton X-100 in microtubule stabilizing buffer (90 s), fixed with 3% formaldehyde, and stained with an anti-α-tubulin antibody, fluorescein-conjugated secondary antibody, and 4,6-diamidino-2-phenylindole (Sigma) (19). Mitotic indices represent counts of at least 100 mitotic cells from three independent experiments.

Results

Microtubule Dynamics in Taxol-Sensitive A549 Cells. A549 cells were injected with rhodamine-labeled tubulin, and the derivatized tubulin was allowed to incorporate into microtubules for 4–6 h before imaging. Fluorescent microtubules in the lamellar regions of the cells were then imaged. The dynamic behavior of microtubules in A549 cells is illustrated in a time-lapse sequence (Fig. 1 and Movies 1 and 2, which are published as supporting information on the PNAS web site, www.pnas.org). The micro-
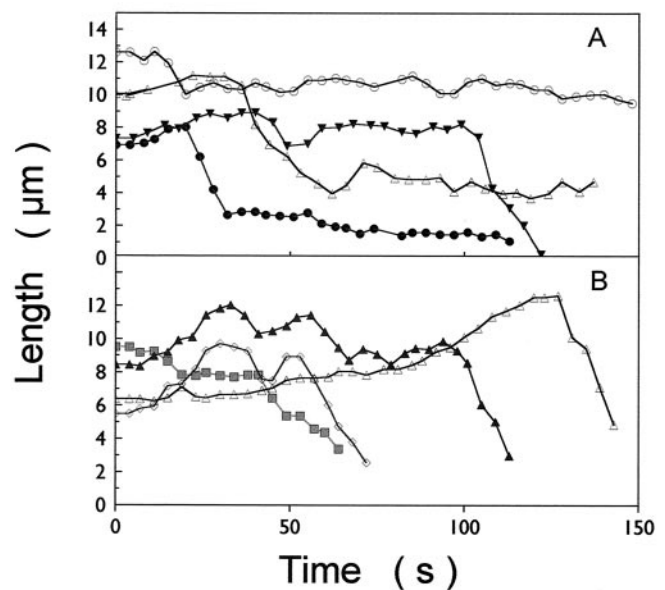

Fig. 2. Life history plots (length changes over a duration of ≈2.5 min) of individual dynamic microtubules in (*A*) A549 cells and (*B*) A549-T12 cells in the absence of added Taxol.

Table 1. Parameters of dynamic instability in the absence of added Taxol

Parameter		A549	A549-T12	% Change[‡]	A549-T24	% Change[‡]
Mean rate,[†] μm/min	Growth	5.2 ± 0.8	6.0 ± 0.5	+15	9.3 ± 1.0***	+79
	Shortening	8.8 ± 0.9	14 ± 1.4**	+59	21 ± 1.9***	+139
Mean length, μm	Growth	1.2 ± 0.1	1.9 ± 0.2***	+58	2.4 ± 0.2***	+100
	Shortening	2.0 ± 0.2	3.5 ± 0.4***	+75	4.6 ± 0.4***	+130
Mean duration, min	Growth	0.34 ± 0.03	0.36 ± 0.03	+6	0.32 ± 0.02	−6
	Shortening	0.27 ± 0.01	0.27 ± 0.02	0	0.28 ± 0.03	+4
	Pause	0.42 ± 0.04	0.30 ± 0.04*	−29	0.31 ± 0.05	−26
% Time spent	Growing	26.7	37.6	+41	37.1	+39
	Shortening	31.9	31.5	−1	37.1	+16
	Pause	41.4	30.9	−25	25.8	−38
Life span, min		2.5 ± 0.1	1.6 ± 0.2***	−36	1.9 ± 0.2**	−24
Dynamicity, μm/min		4.2	6.6	+57	11.2	+167

***, $P < 0.001$; **, $P < 0.005$; *, $P < 0.05$, estimates of significance by Student's t test.
[†]Mean ± SE.
[‡]The percentage difference relative to the corresponding behavioral parameter in A549 cells.

tubules alternated between phases of growing, shortening, and a pause state (a state of attenuated dynamic activity). Life history plots (Fig. 2) of the changes in length over time of individual microtubules clearly illustrate the dynamic behavior of the microtubules. The life history plots of a number of microtubules were used to determine the parameters of dynamic instability (Tables 1 and 2). In A549 cells, microtubules shortened at a mean rate of 8.8 ± 0.9 μm/min, faster than their mean growing rate (5.2 ± 0.8 μm/min). We examined the effects of a low concentration of Taxol (2 nM) on dynamic parameters in interphase A549 cells. Consistent with previous results (6), Taxol decreased the shortening rate (by 41%) and the shortening length (by 40%) but increased the percentage of time paused (by 12%) and suppressed dynamicity, a parameter that reflects the overall dynamics of microtubules (by 28%) (data not shown).

Microtubule Dynamics in Taxol-Resistant Cells. In the absence of added Taxol, microtubule dynamics in the Taxol-resistant cells were significantly greater than in the parental cells. As shown in Fig. 2, Table 1, and Movies 3 and 4, which are published as supporting information on the PNAS web site, microtubules in A549-T12 and -T24 cells incubated for 48 h in Taxol-free medium were significantly more dynamic than those in A549 cells. The greatest changes were: (*i*) the shortening rate increased by 59 and 139% in A549-T12 and -T24 cells (from 8.8 ± 0.9 to 14 ± 1.4 and 21 ± 1.9 μm, respectively); (*ii*) the growth length increased by 58 and 100% (from 1.2 ± 0.1 to 1.9 ± 0.2 and 2.4 ± 0.2 μm, respectively); (*iii*) the shortening length increased by 75 and 130% (from 2.0 ± 0.2 to 3.5 ± 0.4 and 4.6 ± 0.5, respectively); and (*iv*) the total percentage of time spent growing increased by 41 and 39%, respectively. The total time paused decreased significantly, by 25 and 38%, respectively, and the life span of an individual microtubule (the time before complete depolymerization of the microtubule) decreased by 36 and 24%, respectively.

Table 2. Transition frequencies in the absence of added Taxol

Parameter	A549	A549-T12	% Change*	A549-T24	% Change
Catastrophe/min	1.7	1.7	0	2.1	+24
Rescue/min	3.1	2.0	−35	2.2	−29
Catastrophe/μm	1.2	0.59	−51	0.46	−62
Rescue/μm	0.4	0.16	−60	0.13	−68

*The percentage difference relative to the corresponding parameter in A549 cells.

Microtubule dynamic instability is characterized by abrupt stochastic transitions among the phases of growing, shortening, and pause, called "catastrophes" and "rescues." A catastrophe is a transition from the state of growth or pause to shortening, and a rescue is a transition from the shortening state to a state of pause or growth. The number of catastrophes or rescues as measured on the basis of length grown or shortened decreased by 51–68% for both resistant cell lines. The catastrophe frequency per time did not change significantly in A549-T12 cells, although it increased by 24% for the microtubules of A549-T24 cells. In addition, the time-based rescue frequency decreased significantly for both resistant cell lines. Thus, in Taxol-resistant cells, the microtubules shortened and grew faster and for greater lengths than in sensitive A549 cells. They spent less time paused, and the duration of an average pause event was shorter. Dynamicity was increased by 57% in A549-T12 cells and by 167% in A549-T24 cells. Thus the higher the degree of Taxol resistance, the greater the increase in microtubule dynamics in the absence of added Taxol.

Mitotic Block and Spindle Abnormalities Induced by Increased Microtubule Dynamics. In the absence of added Taxol, cells of both resistant lines were blocked in mitosis with major spindle abnormalities. The effects of suppressed microtubule dynamics on mitosis are well known, because all antimitotic drugs examined to date appear to block cells in mitosis by this mechanism (3). However, little is known about the effects of enhanced microtubule dynamics on mitosis. To examine these effects, we determined the mitotic index and spindle organization in A549-T12 cells in the presence and absence of added Taxol. In A549 cells, the mitotic index was 4.7% and in A549-T12 cells maintained in 12 nM Taxol, it was 6.4%. In contrast, removal of Taxol from the medium increased the mitotic index in A549-T12 cells to 22.6%. We examined the distribution of cells in the phases of mitosis to determine at which phase mitosis was blocked. The ratio of cells in anaphase to cells in metaphase decreased from 0.19 in A549-T12 cells maintained in 12 nM Taxol to 0.05 in A549-T12 after Taxol removal (the ratio for the parental A549 cells was 0.32). The results indicate that mitotic block induced in the absence of Taxol occurred specifically at the transition from metaphase to anaphase.

A549-T12 mitotic spindles, in the presence of Taxol, appeared similar to those of parental A549 cells without Taxol; they were bipolar, with chromosomes organized into a compact metaphase plate (compare Fig. 3 *A* and *B* with *D* and *E*). Thirty-three percent of A549-T12 spindles in the presence of Taxol had slight abnormalities with one or two chromosomes near one or both
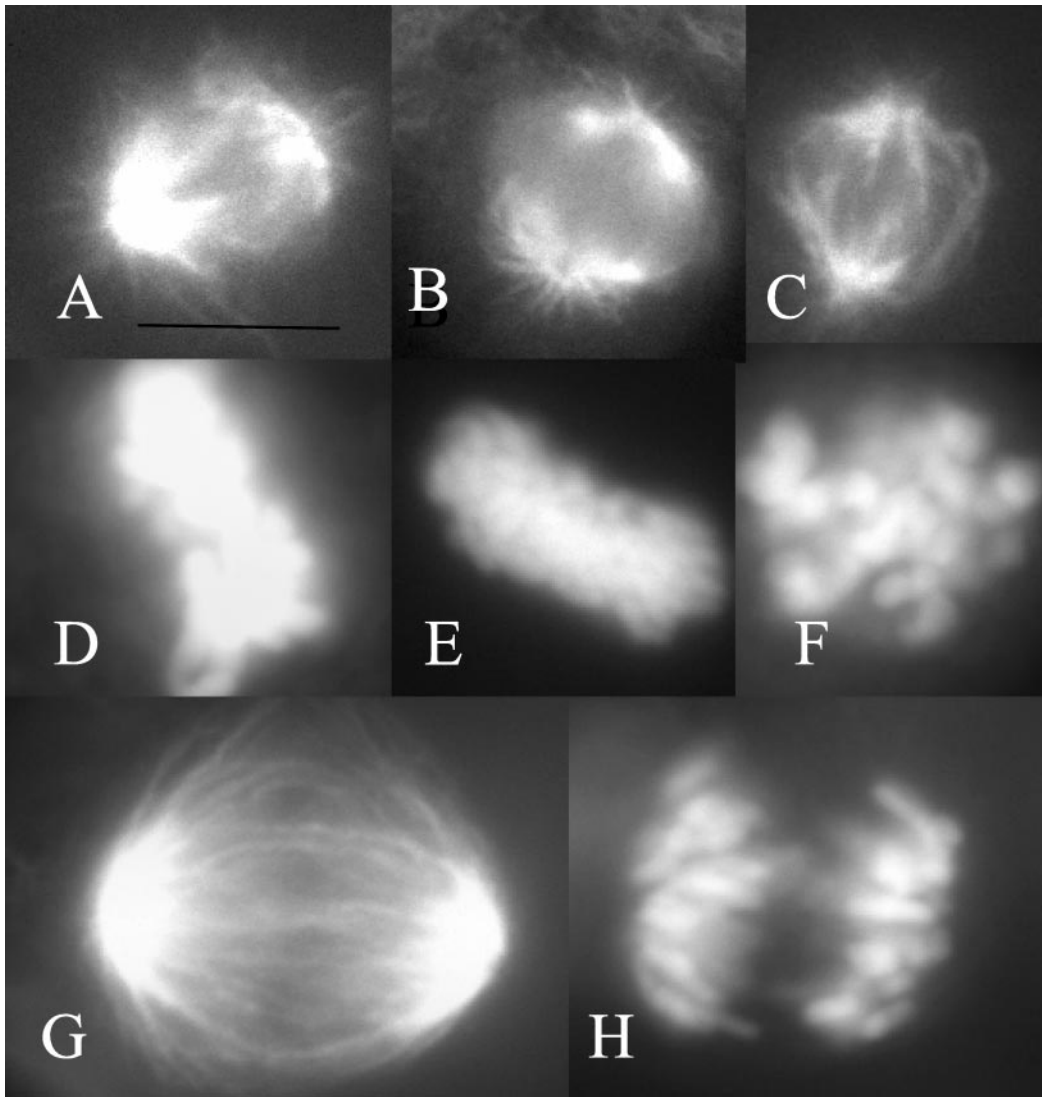
Fig. 3. Mitotic spindle organization. (*A* and *D*) A549 cells; (*B* and *E*) A549-T12 cells in 12 nM Taxol; (*C* and *F*) A549-T12 cells in the absence of added Taxol; (*G* and *H*) anaphase in A549-T12 cells in 12 nM Taxol. (*A–C, G*) Spindle microtubules as shown by antitubulin immunofluorescence. (*D–F, H*) Chromosomes of the same cells as shown by 4,6-diamino-2-phenylindole stain. (Bar = 10 μm.)

poles, rather than being aligned with the majority of the chromosomes at the metaphase plate. There were no ball-shaped spindles or other major alterations, and anaphase occurred normally (Fig. 3 *G* and *H*). However, in the absence of added Taxol, 84% of metaphase spindles in A549-T12 cells were abnormal, displaying either monopolar spindles or bipolar spindles with many uncongressed chromosomes, a decreased density of astral microtubules, and a tendency toward lengthening of the interpolar distance. These spindles appeared skewed or twisted and chromosomes were scattered throughout the spindle as though they had been unable to form stable bipolar microtubule attachments (Fig. 3 *C* and *F*). Anaphase was rare in the absence of added Taxol; when it occurred, spindles were asymmetrical, and distinctly abnormal and chromosomes did not travel together but were spread throughout the cell.

In interphase, microtubules of A549-T12 cells in the presence of Taxol appeared similar to those of the parental cell line (Fig. 4 *A* and *B*) but were more numerous, and there were occasional dense microtubule bundles (arrows). In the absence of Taxol, microtubules in interphase A549-T12 cells were sparse and contorted in conformation (Fig. 4*C*); many of these cells were multinucleated, and some contained apoptotic bodies.

Discussion

We found that, in the absence of added Taxol, the dynamic instability of microtubules of Taxol-resistant A549-T12 and -T24 cells was significantly increased as compared with that of their parental Taxol-sensitive A549 counterparts. The microtubules shortened faster to shorter lengths and grew faster to longer lengths than in the parental cells. Their total life span decreased, and the total time spent paused and the duration of pause events were decreased. For example, in A549-T12 cells in the absence of added Taxol, microtubules shortened 59% faster and lost 75% more of their length during an average shortening event than in the parental A549 cells, and they grew 15% faster and gained 58% more in length than in parental cells. Their overall dynamics were increased by 57%. In the A549-T24 cells, all of the parameters were altered in the direction of an even greater increase in inherent dynamics than in the A549-T12 cells.

Interestingly, the parameters that were altered in the resistant cells corresponded exactly to those that were altered in the opposite way when Taxol was added to cells or to bovine brain microtubules *in vitro* (5, 6). For example, Yvon *et al.* (6) found that 30 nM Taxol suppressed the shortening and growing rates
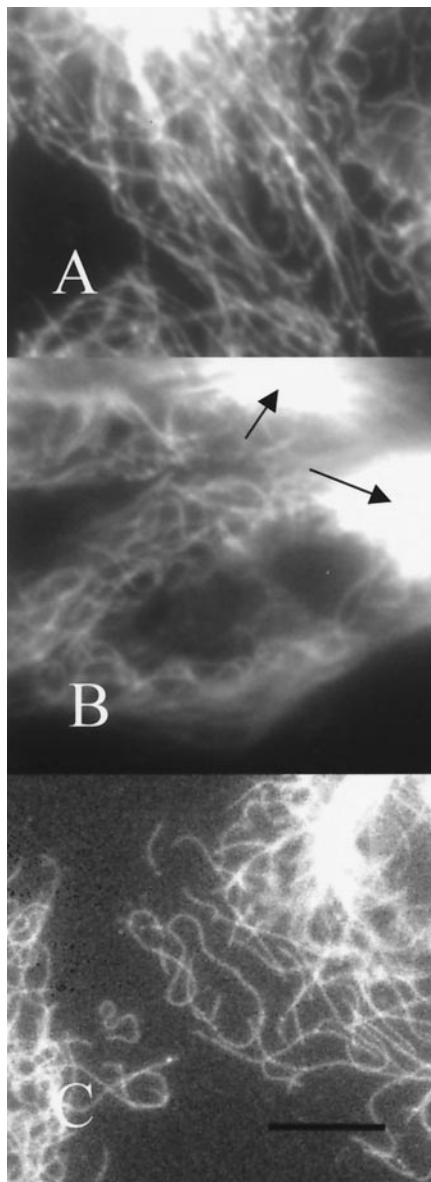
Fig. 4. Microtubule organization in interphase cells. (*A*) A549 cells; (*B*) A549-T12 in 12 nM Taxol; (*C*) A549-T12 in the absence of added Taxol. Antitubulin immunofluorescence. Arrows in *B* point to Taxol-induced microtubule bundles. (Bar = 10 μm.)

apoptosis (9, 10). In addition, chromosomes aligned at the metaphase plate oscillate under tension produced by motor molecules and dynamic kinetochore-attached microtubules. The attachment of a sufficient number of dynamic microtubules to the kinetochores and the resulting development of tension appear to be important in determining signaling by mad2 at the metaphase/anaphase checkpoint (24). The disorganized skewed arrangement of the spindle microtubules and the absence of mature metaphase plates in A549-T12 and -T24 cells in the absence of added Taxol suggests that excessive microtubule dynamics may prevent the stable attachment of sufficient microtubules and/or of balanced numbers of microtubules to sister kinetochores. These abnormalities were essentially corrected in 12 nM Taxol, suggesting that a slowing of microtubule dynamics results in more stable and balanced forces on the kinetochores.

An alternative explanation is that some alteration(s) of the microtubules in the Taxol-resistant cells may make them both more dynamic and unable to attach to the kinetochores of chromosomes except in the presence of Taxol. It is conceivable that such effects might be distinct and not causally related. Taxol clearly affects microtubule structure, because the drug can alter the protofilament structure of microtubules from an average of 13 protofilaments in the absence of Taxol to an average of 12 protofilaments in the presence of Taxol (25, 26). By altering structure, Taxol might inhibit the ability of microtubules to bind to kinetochores. The question also arises whether measurements of microtubule dynamics in the presence and absence of Taxol in interphase cells, as were performed here, truly reflect changes in dynamics in mitotic cells. However, suppression of dynamics of interphase microtubules induced by given concentrations of Taxol (6) and vinblastine (27) correlate very well with mitotic block in the same cell types at the same drug concentrations. Thus, there is a very strong correlation between the effects on interphase microtubule dynamics of two diverse drugs with different microtubule-binding sites and their effects on the progress of cells through mitosis. These observations suggest that changes in dynamics in interphase accurately reflect changes in microtubule dynamics in mitosis. Thus the observations reported here suggest strongly that regulation of microtubule dynamics is an important determinant of successful mitosis.

Interestingly, minor spindle abnormalities with a few uncongressed chromosomes were observed in A549-T12 cells in the presence of Taxol. The significance of this observation is not clear; persistence of mitotic abnormalities in otherwise normally proliferating cells in the presence of Taxol may suggest that some resistant cells have a defective metaphase/anaphase checkpoint, allowing them to survive a slightly abnormal mitosis. Alternatively, the abnormalities may be lethal, reflecting the constant selective pressure of Taxol on the cells.

of microtubules in Caov-3 ovarian carcinoma cells by 32 and 24%, respectively (6). Dynamicity was decreased by 30%. This degree of suppression of microtubule dynamics was associated with complete inhibition of progress into anaphase and complete inhibition of cell proliferation. Enhancement of microtubule dynamics thus appears to be one mechanism by which cells can counteract the inhibitory effects of Taxol on mitosis and proliferation.

Mechanism of Mitotic Block Induced by Increased Microtubule Dynamics. Microtubule dynamics play critical roles in the equipartitioning of chromosomes to the two daughter cells by the mitotic spindle. For example, microtubules emanating from the spindle poles at prometaphase undergo excursions of dynamic instability, probing the cytoplasm until they find and attach to the kinetochores of chromosomes. Failure of the microtubules to capture all of the chromosomes leads to mitotic block and

Why Are Microtubules of A549-T12 and -T24 Cells Highly Dynamic? A number of alterations may conceivably be involved in the enhancement of microtubule dynamics in A549-T12 and -T24 cells, including expression or modification of microtubule-associated proteins (MAPs), mutations in tubulin, or modifications in the balance of tubulin isotypes. Taxol resistance arising from mutations of tubulin genes has been observed previously, although the effects on dynamic instability have not been determined (18, 28, 29). Several MAPs and other microtubule regulatory proteins including MAP4, TOG (tumor overexpressed gene), and stathmin can up- or down-regulate microtubule dynamics, often depending on their phosphorylation states (30–34).

Tubulin isotype composition is also often altered in drug-resistant cell lines (14, 15, 17, 19, 35) and tumor tissue (16). Interestingly, expression of the βIVa-tubulin isotype gene is increased in A549-T12 and -T24 cells, and the βIII-tubulin isotype is overexpressed at the protein level in A549-T24 cells.

In addition, Taxol sensitivity was regained on reduction of the βIII-tubulin isotype by antisense treatment of A549-T24 cells (16, 36). *In vitro*, the isotype composition of microtubules can regulate dynamics in subtle ways. Microtubules assembled from the purified αβIII isotype are considerably more dynamic than microtubules made from the αβII or αβIV isotypes or from unfractionated tubulin (37). In addition, Taxol differentially modulates the dynamics of microtubules assembled from unfractionated and purified β-tubulin isotypes, with microtubules composed of purified αβIV- or αβIII-tubulin being the least drug-sensitive (38).

In conclusion, we find that microtubule dynamic instability is significantly increased in Taxol-resistant/dependent A549 cells. Such an excess of dynamics may contribute to the drug requirement for growth as well as to the drug-resistant phenotype. Thus, these results indicate that microtubule dynamics are a significant factor in drug resistance. Importantly, they provide a rationale for evaluating changes in the biochemical composition of microtubules and their endogenous regulators in tumors as predictive factors for the clinical response to taxane-based chemotherapy. The results also show that microtubule dynamics must be finely regulated for progress through mitosis, and that increased dynamics, as well as suppressed dynamics, result in mitotic block.

1. Crown, J. & O'Leary, M. (2000) *Lancet* **355,** 1176–1178.
2. Schiff, P. B. & Horwitz, S. B. (1980) *Proc. Natl. Acad. Sci. USA* **77,** 1561–1565.
3. Jordan, M. A. & Wilson, L. (1998) *Curr. Opin. Cell Biol.* **10,** 123–130.
4. Horwitz, S. B. (1992) *Trends Pharmacol. Sci.* **13,** 134–136.
5. Derry, W. B., Wilson, L. & Jordan, M. A. (1995) *Biochemistry* **34,** 2203–2211.
6. Yvon, A.-M, Wadsworth, P. & Jordan, M. A. (1999) *Mol. Biol. Cell* **10,** 947–959.
7. Zhai, Y., Kronebusch, P. J., Simon, P. M. & Borisy, G. G. (1996) *J. Cell Biol.* **135,** 202–214.
8. Rusan, N. M., Fagerstrom, C. J., Yvon, A.-M. C. & Wadsworth, P. (2001) *Mol. Biol. Cell* **12,** 971–980.
9. Jordan, M. A., Toso, R. J., Thrower, D. & Wilson, L. (1993) *Proc. Natl. Acad. Sci. USA* **90,** 9552–9556.
10. Jordan, M. A., Wendell, K. L., Gardiner, S., Derry, W. B., Copp, H. & Wilson, L. (1996) *Cancer Res.* **56,** 816–825.
11. Horwitz, S. B., Cohen, D., Rao, S., Ringel, I., Shen, H. J. & Yang, C. P. (1993) *J. Natl. Cancer Inst. Monogr.* **15,** 55–61.
12. Dumontet, C. & Sikic, B. (1999) *J. Clin. Oncol.* **17,** 1061–1070.
13. Minotti, A. M., Barlow, S. B. & Cabral, F. (1991) *J. Biol. Chem.* **266,** 3987–3994.
14. Jaffrezou, J. P., Dumontet, C., Derry, W. B., Duran G., Chen, G., Tsuchiya, E., Wilson. L., Jordan, M. A. & Sikic, B. I. (1995) *Oncol. Res.* **7,** 517–527.
15. Dumontet, C., Duran, G. E., Steger, K. A., Beketic-Oreskovic, L. & Sikic, B. I. (1996) *Cancer Res.* **56,** 1091–1097.
16. Kavallaris, M., Kuo, D.Y.-S., Burkhart, C. A., Regl, D. L., Norris, M. D., Haber, M. & Horwitz, S. B. (1997) *J. Clin. Invest.* **100,** 1282–1293.
17. Haber, M., Burkhart, C. A., Regl, D. L., Madafiglio, J., Norris, M. D. & Horwitz, S. B. (1995) *J. Biol. Chem.* **270,** 31269–31275.
18. Giannakakou, P., Sackett, D. L., Kang, Y. K., Zhan, Z., Buters, J. T., Fojo, T. J. & Poruchynsky, M. S. (1997) *J. Biol. Chem.* **272,** 17118–17125.
19. Carles, G., Braguer, D., Dumontet, C., Bourgarel, V., Gonçalves, A., Sarrazin, M., Rognoni, J. B. & Briand, C. (1999) *Br. J. Cancer* **80,** 1162–1168.
20. Monzo, M., Rosell, R., Sanchez, J. J., Lee, J. S., O'Brate, A., Gonzales-Larriba, J. L., Alberola, V., Lorenzo, J. C., Nunez, L., Ro, J. Y. & Martin, C. (1999) *J. Clin. Oncol.* **17,** 1786–1793.
21. Martello, L. A., McDaid, H. M., Regl, D., Yang, C.-P. H., Meng, D., Pettus, T. R. R., Kaufman, M. D., Arimoto, H., Danishefsy, S. J., Smith, A. B., III, & Horwitz, S. B. (2000) *Clin. Cancer Res.* **6,** 1978–1987.
22. Hyman, A., Drechsel, D., Kellogg, D., Salser, S., Sawin, K., Steffen, P., Wordeman, L. & Mitchison, T. (1991) *Methods Enzymol.* **196,** 478–485.
23. Walker, R. A., O'Brien, E. T., Pryer, N. K., Soboeiro, M. F., Voter, W. A., Erickson, H. P. & Salmon, E. D. (1988) *J. Cell Biol.* **107,** 1437–1448.
24. Gorbsky, G. J. (1997) *BioEssays* **19,** 193–197.
25. Mogenson, M. M. & Tucker, J. B. (1990) *J. Cell Sci.* **97,** 101–107.
26. Andreu, J. M., Bordas, J., Diaz, J. F., Garcia de Ancos, J., Gil, R., Medrano, F. J., Nogales, E., Pantos, E. & Towns-Andrews, E. (1992) *J. Mol. Biol.* **226,** 169–184.
27. Dhamodharan, R. I., Jordan, M. A., Thrower, D., Wilson, L. & Wadsworth, P. (1995) *Mol. Biol. Cell.* **6,** 1215–1229.
28. Cabral, F. R., Abraham, I. & Gottesman, M. M. (1981) *Proc. Natl. Acad. Sci. USA* **78,** 4388–4391.
29. Gonzalez-Garay, M. L., Chang, L., Blade, K., Menick, D. R. & Cabral, F. (1999) *J. Biol. Chem.* **274,** 23875–23882.
30. Toso, R. J., Jordan, M. A., Farrell, K. W., Matsumoto, B. & Wilson, L. (1993) *Biochemistry* **32,** 1285–1293.
31. Dhamodharan, R. & Wadsworth, P. (1995) *J. Cell. Sci.* **108,** 1679–1689.
32. Vasquez, R. J., Gard, D. L. & Cassimeris, L. (1994) *J. Cell Biol.* **127,** 985–993.
33. Ookata, K., Hisanaga, S., Bulinski, J. C., Murofushi, H., Aizawa, H., Itoh, T. J., Hotani, H., Okumura, E., Tachibana, K. & Kishimoto, T. (1995) *J. Cell. Biol.* **128,** 849–862.
34. Andersen, S. S. L. (2000) *Trends Cell Biol.* **10,** 261–267.
35. Ranganathan, S., Dexter, D. W., Benetatos, C. A., Chapman, A. E., Tew, K. D. & Hudes, G. R. (1996) *Cancer Res.* **56,** 2584–2589.
36. Kavallaris, M., Burkhart, C. A. & Horwitz, S. B. (1999) *Br. J. Cancer* **80,** 1020–1025.
37. Panda, D., Miller, H. P., Banerjee, A., Luduena, R. F. & Wilson, L. (1994) *Proc. Natl. Acad. Sci. USA* **91,** 11358–11362.
38. Derry, W. B., Wilson, L., Khan, I. A., Luduena, R. F. & Jordan, M. A. (1997) *Biochemistry* **36,** 554–562.

Gonçalves *et al.*